The Voyager 2 Encounter with the Uranian System

E. C. Stone and E. D. Miner

An overview of the Voyager 2 encounter with Uranus is presented, including a brief discussion of the trajectory and the planned observations as well as the highlights of the results described in the 11 companion papers.

With the successful accomplishment of its encounter with Uranus, Voyager 2 completed the fifth step in the NASA Voyager program of exploration of the outer planets, which began with the launch of Voyager 2 from Cape Canaveral, Florida, on 20 August 1977 (*1*). Before the closest approach of Voyager 2 to Uranus on 24 January 1986, both Voyager 1 and Voyager 2 had completed successful encounters with Jupiter [closest approaches, 5 March and 9 July 1979, respectively (*2*)] and with Saturn [closest approaches, 12 November 1980 and 26 August 1981, respectively (*3*)]. Voyager 2 is the first spacecraft to have flown through the Uranian system, and, barring catastrophic failures, it will be the first to encounter Neptune and Triton in late August 1989. This and the following reports summarize the initial findings from the investigations conducted during the Voyager 2 passage through the Uranian system.

The investigations and principal investigators are listed in Table 1. All instruments and engineering systems, including the science instrument scan platform (which seized temporarily during the Saturn encounter), functioned nominally during the encounter with Uranus. Platform usage was limited to low rates because extensive laboratory and spacecraft testing showed that these were far less likely to cause seizure than the high rate used at Saturn. Although contingency back-up sequences and procedures were prepared in the event of scan platform seizure and other problems, none of these was required during the mission.

Several improvements were made to the spacecraft and ground systems since the 1981 Saturn encounter. Attitude control was altered to reduce angular rates by a factor of 2 or 3 and to compensate better for impulses from tape recorder starts and stops; this resulted in images with much less smear than those obtained during Jupiter and Saturn encounters. Satellite pictures also benefited from improvement and extensive use of target motion compensation, in which the entire spacecraft was slowly rotated to keep the cameras pointed at a nearby satellite. On-board image data compression by the back-up flight data system computer reduced real-time imaging data rates by almost 70%. Data were encoded with the Reed-Solomon encoder, an item of hardware launched with Voyager but not used for any previous encounters. Ground-tracking stations were frequently arrayed to provide an effectively larger collector for the weak spacecraft signal. The Parkes Radio Telescope in Australia was made available to enhance the capability of the Canberra Deep Space Network (DSN) tracking station during critical data-gathering periods. That all of this worked so well testifies to the high level of expertise and the spirit of teamwork within the Voyager project and supporting organizations.

Although the flyby distance at Uranus was chosen to deflect the spacecraft toward Neptune, the timing of the encounter was chosen to provide a close approach to Miranda and to place the periods of planet and ring radio occultation in coincidence with the center of the tracking pass at Canberra; because of Uranus' southerly declination, this station was well suited for high-quality, long-duration collection of Voyager radio science data. Voyager 2's path through the satellite system of Uranus is shown in Fig. 1.

Voyager 2 encounter activities commenced on 4 November 1985, with the spacecraft 10.3 million kilometers from Uranus. Closest approach, at 107,000 km from the center of Uranus, occurred at 1759 U.T.C. (coordinated universal time) on 24 January 1986. The encounter period ended on 25 February 1986.

The design of the Uranus science sequences relied primarily on telescopic observations from Earth, although some early Voyager data were used to make revisions to later observations. For example, one image of Miranda was diverted to 1985U1 to obtain a closer view of this small satellite after it was discovered by Voyager in late December 1985.

Ring occultations of σ Sagittarii and β Persei were observed by the photopolarimeter (PPS) and the ultraviolet spectrometer (UVS). Radio science (RSS) data were collected in Australia during a 4-hour period that included occultation, but not extinction, of the spacecraft signal by the rings and the planet. γ Pegasi and ν Geminorum occultations by Uranus were also observed by UVS. Special observations by the imaging system (ISS) provided close-up color pictures of the five previously known satellites and higher resolution black-and-white pictures of four of them. The temperature of Uranus' atmosphere was mapped with the infrared interferometer spectrometer (IRIS), and PPS, ISS, IRIS, and UVS were used to determine the scattering, emitting, and reflecting characteristics of the atmosphere under various viewing conditions.

Table 1. Voyager investigations and principal investigators.

Investigation	Principal investigator and affiliation
Imaging system (ISS)	B. A. Smith, University of Arizona, Tucson, AZ
Photopolarimetry (PPS)	A. L. Lane, Jet Propulsion Laboratory, California Institute of Technology, Pasadena, CA
Infrared interferometer spectroscopy (IRIS)	R. A. Hanel, Goddard Space Flight Center, Greenbelt, MD
Ultraviolet spectroscopy (UVS)	A. L. Broadfoot, University of Arizona, Tucson, AZ
Radio science (RSS)	G. L. Tyler, Stanford University, Stanford, CA
Magnetometry (MAG)	N. F. Ness, Goddard Space Flight Center, Greenbelt, MD
Plasma (PLS)	H. S. Bridge, Massachusetts Institute of Technology, Cambridge, MA
Low-energy charged particles (LECP)	S. M. Krimigis, Applied Physics Laboratory, Johns Hopkins University, Baltimore, MD
Cosmic ray (CRS)	E. C. Stone, California Institute of Technology, Pasadena, CA
Planetary radio astronomy (PRA)	J. W. Warwick, Radiophysics Inc., Boulder, CO
Plasma waves (PWS)	F. L. Scarf, TRW Defense and Space Systems Group, Redondo Beach, CA

E. C. Stone, Division of Mathematics, Physics, and Astronomy, California Institute of Technology, Pasadena, CA 91125.
E. D. Miner, Jet Propulsion Laboratory, California Institute of Technology, Pasadena, CA 91109.

Ring images were obtained on approach to the planet, near the time of ring plane crossing, while the rings were silhouetted against the illuminated atmosphere, and during passage of the spacecraft through the shadow of Uranus. Images were also obtained as the spacecraft was receding from the dark side of the planet. Extensive searches for new satellites were conducted by ISS, both within and exterior to the ring system. The spacecraft was rolled to a specific orientation during the final few hours of approach to the planet to enhance observations of any corotating ions or plasma by the plasma (PLS) and low-energy charged-particle (LECP) experiments. High-rate plasma wave (PWS) and planetary radio astronomy (PRA) data were recorded to search for tiny ring particles during ring plane crossing 43 minutes before closest approach to Uranus. The magnetosphere and its charged-particle population were observed continuously by the magnetometer (MAG) and cosmic ray (CRS) experiments as well as by LECP and PLS.

Atmosphere. Although Uranus apparently lacks a large internal heat source, and although the sun directly heats the polar regions, its atmosphere nevertheless bears a resemblance to those of Jupiter and Saturn. At a pressure of 600 mbar, temperatures at the poles and the equator are essentially the same, indicating some means of dynamical redistribution of the solar energy deposited in the polar regions. In contrast to Jupiter and Saturn, however, slightly colder bands exist at approximately 25°S and 40°N. At higher altitudes (100-mbar pressure), the temperature drops to a minimum of 52 ± 2 K before increasing to 750 K in the extreme upper atmosphere. A multilayer ionosphere is found at an altitude of 2000 to 3500 km above 100 mbar and may extend to altitudes of more than 10^4 km. A hydrogen corona extends out beyond the rings; this corona has a density of 100 cm^{-3} at the ϵ ring.

The mole fraction of atmospheric helium is 0.15 ± 0.05; this is somewhat greater than that at Jupiter and Saturn but is consistent with the solar helium abundance. In the upper atmosphere there is also a trace of methane, which absorbs in the red and gives Uranus its blue-green appearance. The signature of a cloud deck of methane ice at pressures of 900 to 1300 mbar was evident from initial study of the radio occultation data, indicating a methane mole fraction deeper in the atmosphere of about 2%. This value is 20 times the solar carbon abundance, as might be expected from the ice-rich material that originally formed Uranus.

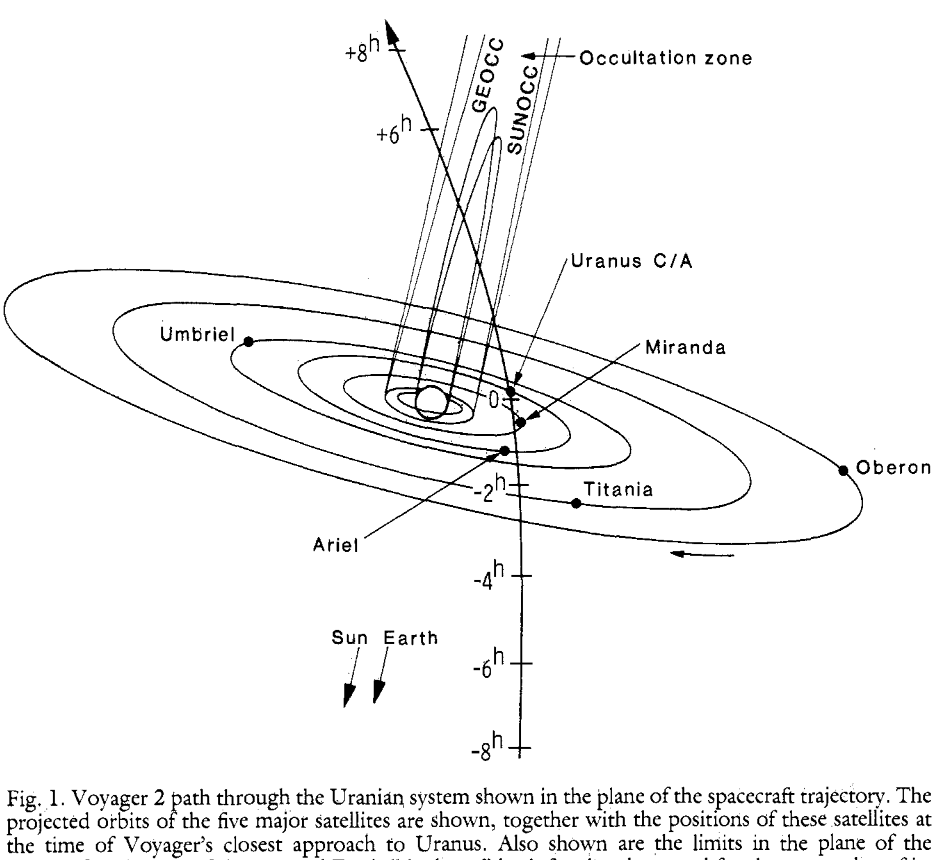

Fig. 1. Voyager 2 path through the Uranian system shown in the plane of the spacecraft trajectory. The projected orbits of the five major satellites are shown, together with the positions of these satellites at the time of Voyager's closest approach to Uranus. Also shown are the limits in the plane of the spacecraft trajectory of the sun and Earth "shadows," both for the planet and for the outer edge of its rings. Tick marks along the trajectory indicate Voyager's position at 2-hour intervals. GEOCC, Earth occultation; SUNOCC, sun occultation; Uranus C/A, Voyager closest approach to Uranus.

At approximately 50°S, the methane clouds appear as bands with a 700-km latitudinal scale, suggesting discrete sources and little latitudinal diffusion. At lower latitudes there are individual convective plumes of methane ice having prograde velocities of 40 to 160 m sec^{-1} relative to the interior of the planet, which has a rotation period of 17.24 hours as determined from the periodic radio emissions. The direction of these winds is opposite that of the thermal winds expected from the observed latitudinal termperature gradient, indicating the presence of other dynamical processes. The importance of planetary rotation to atmospheric dynamics is further illustrated by the appearance of zonal bands in the polar haze, which is photochemically produced from methane.

At higher altitudes, intense ultraviolet light is emitted almost uniformly from the sunlit hemisphere. This emission is due to electroglow, a radiative process first observed at Jupiter and Saturn. Excited by low-energy electrons [$kT \sim 3$ eV at Uranus (k, Boltzmann constant; T, temperature in kelvins)], the emission occurs well above the homopause and consists of both molecular and atomic hydrogen emissions. The electroglow process, which could possibly be driven by the coupling of atmospheric winds into the ionosphere, also produces 10^{29} hydrogen atoms per second by H_2 dissociation. Half of the atomic hydrogen escapes, contributing to the extended hydrogen corona.

Auroral emissions were also observed on the dark side of Uranus. These emissions are produced by the excitation of H_2 by approximately 10-keV electrons and form an auroral region 15° to 20° in diameter about the magnetic pole.

Rings. The characteristics of Uranus' rings offer the prospect of a better understanding of the origin of ring systems and their associated dynamical processes. Some of the physical characteristics are given in Table 2, which includes 1986U1R and 1986U2R, two new rings discovered in Voyager images. 1986U1R is a narrow ring similar to the others; 1986U2R is broad and diffuse. A number of other possible rings or partial rings (arcs) have been identified in stellar occultation data. The spectral reflectance of the individual ring particles is low (<5%), and at least the ϵ ring is gray. Color images show no statistically significant color differences between the ϵ and other rings.

It was expected that there would be up to 18 small satellites (shepherds) confining the narrow rings between them. Two such shepherd satellites, 1986U7 and 1986U8, were found on either side of the ϵ ring (Table 3). The outer edge of the ϵ ring, which is quite sharp, closely corresponds to

Table 2. Uranus ring data. Values in parentheses are uncertain.

Feature	Distance from Uranus center (10^3 km)	Eccentricity (10^{-3})	Inclination (10^{-3} degrees)	Width (km)†	Mean visual optical depth†	Maximum radio optical depth†
1986U2R	37–39.5	0?	0?	~2500	0.001–0.0001	
6 ring	41.85*	1.0*	63*	1–3	0.2–0.3	0.8–1.1
5 ring	42.24*	1.9*	52	2–3	0.5–0.6	1.2–2.3
4 ring	42.58*	1.1*	32*	2–3	0.3	1.2–1.5
α	44.73*	0.8*	14*	7–12	0.3–0.4	1.0–2.5
β	45.67*	0.4*	5*	7–12	0.2	0.5–1.0
η	47.18*	(0)*	(2)*	0–2	0.1–0.4	0.7–1.1
γ	47.63*	(0)*	(11)*	1–4	1.3–2.3	3.8–6.9
δ	48.31*	(0)*	4*	3–9	0.3–0.4	1.2–4
1986U1R	50.04	0?	0?	1–2	0.1	
ε	51.16*	7.9*	(1)*	22–93	0.5–2.1	2.5–8

*Data from (*4*). †Ring widths and optical depths vary greatly with ring longitude.

the location of a high wavenumber resonance of 1986U8, and the inner edge is close to a similar resonance of 1986U7. Because these resonances do not overlap, the interaction is the same as that between Mimas and the outer edge of Saturn's B ring and differs from the shepherding interaction at Saturn's narrow F ring. Shepherd satellites for the other Uranian rings were not found, probably because they are too small (<14 km in diameter) and are charcoal black like the ring particles.

Surprisingly, particles smaller than tens of centimeters were absent from the ε ring, as evidenced by the similarity of the optical thickness of the ring at different radio and optical wavelengths. The sharp edge of the ε ring indicates a ring edge thickness less than 150 m. The relative paucity of smaller particles may be the result of atmospheric drag from the extended hydrogen atmosphere.

A long-exposure image at high phase angle did reveal a broad but optically thin distribution of micrometer-size particles inward from the orbit of 1986U1R to at least the outer edge of 1986U2R. The dust distribution is highly structured, most closely resembling Saturn's D ring. There is also evidence from impacts on the spacecraft as it passed through the ring plane of a 4000-km-thick band of micrometer-size dust particles 116,000 km from the center of the planet. The maximum impact rate detected by the plasma wave instrument was 20 to 30 $\sec^{-1}$, corresponding to a maximum number density of approximately 0.001 m^{-3}.

Several of the main rings exhibit striking variability in opacity with longitude. Both the δ and γ rings vary by more than a factor of 2 in width, and the narrow component of the η ring completely disappears in places. This longitudinal variability in the main rings and the possible presence of numerous adjacent ring arcs suggest that Uranus' rings are dynamic and may be young, rather than having formed at the same time as Uranus.

Satellites. Ten new satellites were found in Voyager images to be orbiting between Uranus and Miranda. Their orbital and physical characteristics, as well as those of the five major satellites of Uranus, are summarized in Table 3. Voyager 2 provided the first disk-resolved images of these distant moons. As expected, the five major satellites are in synchronous rotation, with one side always facing Uranus; it is presumed that the ten newly discovered satellites are also in locked rotation. All 15 satellites are in nearly circular orbits, and, with the exception of Miranda, all orbit in the Uranus equatorial plane.

The mass of the Uranian system, expressed as the product of mass and the universal gravitational constant (G), was found from radio tracking data to be 5,794,547 ± 60 $km^3 \sec^{-2}$. As determined from a combination of radio and optical navigation data, the mass of Uranus itself is 5,793,939 ± 60 $km^3 \sec^{-2}$, with the difference of 608 ± 60 $km^3 \sec^{-2}$ being contained almost entirely in the five major satellites. The mass of Miranda was determined from changes in the Doppler velocity of the spacecraft as it passed within 28,260 km of the satellite; the masses of the other four major satellites were determined from a combination of radio tracking and optical navigation data. These data gave the densities of the satellites listed in Table 3. The densities show no obvious trend with orbital radius. At least the outer four satellites have significantly higher densities than the Saturnian satellites of comparable size, implying that they have a smaller fraction of water ice in their interiors than their Saturnian counterparts.

Oberon and Umbriel appear to have the oldest surfaces. These moons show numerous large impact craters and little evidence for surface changes since the end of an early cratering epoch that probably involved bombardment by debris from outside the Uranian system. However, the dark patches on the floors of some of the craters on

Table 3. Uranus satellite data.

Satellite name	Diameter (km)	Distance from Uranus center (10^3 km)	Orbital period (hours)	$G \times$ mass ($km^3 \sec^{-2}$)	Density ($g\ cm^{-3}$)	Normal albedo
1986U7	~40*	49.7	8.0			<0.1*
1986U8	~50*	53.8	9.0			<0.1*
1986U9	~50*	59.2	10.4			<0.1*
1986U3	~60*	61.8	11.1			<0.1*
1986U6	~60*	62.7	11.4			<0.1*
1986U2	~80*	64.6	11.8			<0.1*
1986U1	~80*	66.1	12.3			<0.1*
1986U4	~60*	69.9	13.4			<0.1*
1986U5	~60*	75.3	14.9			<0.1*
1985U1	170 ± 10	86.0	18.3			0.07 ± 0.02
Miranda	484 ± 10	129.9	33.9	5.0 ± 1.5	1.26 ± 0.39	0.34 ± 0.02
Ariel	1160 ± 10	190.9	60.5	90 ± 16	1.65 ± 0.30	0.40 ± 0.02
Umbriel	1190 ± 20	266.0	99.5	85 ± 16	1.44 ± 0.28	0.19 ± 0.01
Titania	1610 ± 10	436.3	208.9	232 ± 12	1.59 ± 0.09	0.28 ± 0.02
Oberon	1550 ± 20	583.4	323.1	195 ± 11	1.50 ± 0.10	0.24 ± 0.01

*These minor satellite diameters represent upper limits; the corresponding normal albedos calculated from these diameters are thus lower limits but are probably lower than the listed upper limits of 0.1.

Oberon must have formed later, and it is possible that the darkness of Umbriel's surface may represent a more recent coating of low albedo dust and small debris somehow created near and confined to the vicinity of Umbriel's orbit.

The other major satellites show increasingly diverse geological features across their surfaces with decreasing orbital distance. Although Oberon and Umbriel display dense populations of large craters, Titania's surface is covered with craters 10 to 50 km in diameter. These probably formed during a later bombardment by objects in orbit about Uranus. Only two or three larger craters remain. Titania's surface also shows an extensive series of fault scarps having vertical relief of 2 to 5 km, several of which expose brighter material.

Ariel has the brightest and geologically youngest surface in the Uranian satellite system. Here, too, craters larger than about 50 km are for the most part absent. Surface faults are more universal in their extent than those on Titania, and there is evidence for icy flows on portions of the surface.

Miranda is the smallest and innermost of Uranus' major satellites. Its surface, much of which was imaged at resolutions of a kilometer or less, consists of undulating cratered plains with little albedo contrast and trapezoidal to ovoid regions patterned by subparallel sets of mostly dark and a few bright bands, somewhat resembling racetracks. One of these banded regions contains a bright, chevron-shaped feature with sharp corners that is probably of internal origin. In some regions there are scarps with slope lengths of 20 km and graben 10 to 15 km deep. There are some similarities between the ridges and valleys of Miranda and the grooved terrain of Jupiter's Ganymede, but the origin of these features is not well understood.

The high degree and large diversity of the tectonic activity on Miranda is surprising, given its small size and low temperature (86 ± 1 K). Some additional heat source, such as tidal heating, must have taken part along with some means of mobilizing the flow of icy material at low temperatures. The presence of brighter material in the trapezoidal and ovoid regions suggests a possible enrichment of volatiles in these regions that may have contributed to the tectonic processes.

Surface reflectivity of the satellites also shows no trend with orbital radius, except that the minor satellites, which are inside the orbit of Miranda, are much darker than the major satellites, with albedos of less than 10%. Ariel (albedo, 0.40 ± 0.02) is the brightest of the major satellites; Umbriel (albedo, 0.19 ± 0.01) is the darkest. Umbriel also has the lowest contrast across its surface.

The extreme darkness of the small satellites and the rings of Uranus may be due to a greater concentration of the same dark material present on the surfaces of the larger satellites. 1985U1, the largest of the newly discovered satellites, was imaged from 500,000 km and has an albedo of about 7%. This 170-km body is nearly spherical, displays a few muted craters, and has no discernible albedo contrast across its surface. The darkness of the rings and small satellites may indicate the presence of carbonaceous material, or it may result from the high-energy proton bombardment of methane trapped in their icy surfaces.

Magnetosphere. The first direct indication of a Uranian magnetic field was from radio emissions detected 5 days before closest approach, at a distance of about 275 Uranus radii (R_U). Voyager subsequently crossed a well-defined, detached bow shock at 23.5 R_U and entered a fully developed magnetosphere at 18 R_U, revealing a magnetic dipole field with an axis at an unexpectedly large angle of 60° with respect to the rotation axis of the planet and offset from the center of Uranus by 0.3 R_U. The dipole moment is 0.23 G $R_U{}^3$, giving a surface magnetic field ranging from 0.1 to 1.1 G. The intensity of the field and its offset suggest that it is generated at an intermediate depth where water may be under sufficient pressure to be electrically conductive. The rotation period of the magnetic field, which is presumed to be that of this interior region, is 17.24 ± 0.01 hours.

The dipole field is deformed by the incident solar wind, resulting in a magnetotail geometry similar to that at Earth. The tail has a radius of 42 R_U at a distance of 67 R_U behind Uranus and has a plasma sheet approximately 10 R_U thick. Because the planetary rotation axis is directed essentially sunward at this time in the Uranian year, the magnetotail rotates about the antisun line with the same period as the planet.

Within the magnetosphere, there is an extensive distribution of charged particles (mainly hydrogen ions and electrons). There are two principal plasma ion populations, a warm ($\sim$10 eV) component within about 7 R_U that has a maximum density of 2 cm^{-3} planetward of Miranda's orbit, and a hot component ($\sim$1000 eV) confined outside about 5 R_U. Ionization of the extended hydrogen corona may be the major source of the plasma, although the ionosphere and the solar wind may also be sources. The energy density of the plasma is small compared to that of the magnetic field.

The orientation of the rotation axis results in sunward convection of the plasma, which is fundamentally different from that in the magnetospheres of Jupiter and Saturn, in which radial transport is dominated by diffusion. The rapid convective time scale of approximately 40 hours may preclude the accumulation of a significant density of heavy ions sputtered from the satellite surfaces.

The trapped ion population at higher energies outside Miranda's orbit is also dominated by protons, with spectra characterized by temperatures of 4 to 30 keV, although non-Maxwellian tails to the spectra extend to more than 10 MeV. The proton fluxes are too small to cause significant distortion of the magnetic field, but they are large enough to modify and darken any methane on the satellite surfaces in less than 100,000 years.

Energetic electrons with temperatures greater than 20 keV are observed throughout the magnetosphere, terminating abruptly at about 18 R_U on the dark side of the planet where the magnetotail begins. The approximately 1-MeV electron fluxes peak inside Miranda's orbit because of the adiabatic acceleration that occurs as the electrons diffuse radially inward from the outer magnetosphere. Intense whistler-mode hiss and chorus emissions are present inside 8 R_U; these radio emissions cause electron precipitation, which in turn may contribute to nightside ultraviolet emissions.

Both proton and electron fluxes are strongly absorbed by Miranda, Ariel, and Oberon, with the largest effects appearing at high energies. Because of the extreme tilt of the magnetic dipole, the satellites sweep across a broad range of magnetic latitudes as the planet rotates, possibly producing a strong latitude variation in the trapped radiation. Other satellite-related effects may include narrowband plasma waves and emissions of an unknown nature detected near Miranda's orbit.

There are also radio emissions from Uranus, although of lower average power than that at Saturn and therefore detectable only near the planet. The radio emissions are left-hand polarized and have maximum power when the negative magnetic pole, which is currently on the dark side, is tipped toward the spacecraft. When observed from the dayside, the peak frequency is approximately 60 kHz; nightside emissions extend up to 800 kHz, suggesting that a large day-night asymmetry in the density of the plasmasphere may be affecting the propagation of the radio waves.

Summary. As detailed analysis of the results from the Voyager 2 Uranus encounter progresses over the next few years, our understanding of Uranus and its rings, moons, and magnetosphere will continue to grow. In the meantime, the two Voyager spacecraft will continue to explore the interplanetary medium, perhaps encountering the heliopause. If the spacecraft continue to operate as well in the future as they have in the past, they might continue to transmit data until well into the 21st century, when their radioisotope thermoelectric power output will eventually drop to levels that are insufficient to permit spacecraft operation.

REFERENCES AND NOTES

1. For a discussion of the spacecraft, mission design criteria, trajectory selection, and the scientific investigations, see *Space Sci. Rev.* **21**, 75 (1977); *ibid.*, p. 235. A description of the design of the Voyager spacecraft is given in R. F. Draper, W. I. Purdy, G. Cunningham, paper 75-1155 presented at the American Institute of Aeronautics and Astronautics–American Geophysical Union Conference on the Exploration of the Outer Planets, St. Louis, MO, 17–19 September 1975.
2. Voyager 1 Jupiter results are outlined in *Science* **204**, 945–1008 (1979); *Nature (London)* **280**, 725–806 (1979); *Geophys. Res. Lett.* 7, 1–68 (1980). Voyager 2 Jupiter results are outlined in *Science* **206**, 925–996 (1979). Combined Voyager Jupiter results are contained in *J. Geophys. Res.* **85**, 8123—8841 (1981).
3. Voyager 1 Saturn results are outlined in *Science* **212**, 159–243 (1981); *Nature (London)* **292**, 675–755 (1981). Voyager 2 Saturn results are outlined in *Science* **215**, 499–594 (1982). Combined Voyager Saturn results are contained in *J. Geophys. Res.* **88**, 8625–9018 (1983). See also two special Saturn issues of *Icarus* [**52**, no. 2 (1983); **54**, no. 2 (1983)]; T. Gehrels and M. S. Matthews, Eds., *Saturn* (Univ. of Arizona Press, Tucson, 1984); R. Greenberg and A. Brahic, Eds., *Planetary Rings* (Univ. of Arizona Press, Tucson, 1984).
4. R. G. French, J. L. Elliot, E. E. Levine, in preparation.

5. We wish to pay special tribute to the members of the Voyager project team, without whom the data reported in these papers could not have been collected. The Voyager program is one of the programs of the Solar System Exploration Division of NASA's Office of Space Science and Applications. The Voyager project is managed by the Jet Propulsion Laboratory of the California Institute of Technology under NASA contract NAS7-918.

14 April 1986; accepted 5 May 1986

Voyager 2 in the Uranian System: Imaging Science Results

B. A. Smith, L. A. Soderblom, R. Beebe, D. Bliss, J. M. Boyce, A. Brahic, G. A. Briggs, R. H. Brown, S. A. Collins, A. F. Cook II, S. K. Croft, J. N. Cuzzi, G. E. Danielson, M. E. Davies, T. E. Dowling, D. Godfrey, C. J. Hansen, C. Harris, G. E. Hunt, A. P. Ingersoll, T. V. Johnson, R. J. Krauss, H. Masursky, D. Morrison, T. Owen, J. B. Plescia, J. B. Pollack, C. C. Porco, K. Rages, C. Sagan, E. M. Shoemaker, L. A. Sromovsky, C. Stoker, R. G. Strom, V. E. Suomi, S. P. Synnott, R. J. Terrile, P. Thomas, W. R. Thompson, J. Veverka

Voyager 2 images of the southern hemisphere of Uranus indicate that submicrometer-size haze particles and particles of a methane condensation cloud produce faint patterns in the atmosphere. The alignment of the cloud bands is similar to that of bands on Jupiter and Saturn, but the zonal winds are nearly opposite. At mid-latitudes ($-70°$ to $-27°$), where winds were measured, the atmosphere rotates faster than the magnetic field; however, the rotation rate of the atmosphere decreases toward the equator, so that the two probably corotate at about $-20°$. Voyager images confirm the extremely low albedo of the ring particles. High phase angle images reveal on the order of 10^2 new ringlike features of very low optical depth and relatively high dust abundance interspersed within the main rings, as well as a broad, diffuse, low optical depth ring just inside the main ring system. Nine of the newly discovered small satellites (40 to 165 kilometers in diameter) orbit between the rings and Miranda; the tenth is within the ring system. Two of these small objects may gravitationally confine the ϵ ring. Oberon and Umbriel have heavily cratered surfaces resembling the ancient cratered highlands of Earth's moon, although Umbriel is almost completely covered with uniform dark material, which perhaps indicates some ongoing process. Titania and Ariel show crater populations different from those on Oberon and Umbriel; these were probably generated by collisions with debris confined to their orbits. Titania and Ariel also show many extensional fault systems; Ariel shows strong evidence for the presence of extrusive material. About half of Miranda's surface is relatively bland, old, cratered terrain. The remainder comprises three large regions of younger terrain, each rectangular to ovoid in plan, that display complex sets of parallel and intersecting scarps and ridges as well as numerous outcrops of bright and dark materials, perhaps suggesting some exotic composition.

Voyager 2 acquired approximately 7000 images of Uranus, its rings, and its satellites during the several months surrounding the spacecraft's closest approach to Uranus in late January 1986. Images of the Uranian system were more difficult to acquire than those of Jupiter and Saturn for several reasons. Because of the low light levels [Uranus is about 19 astronomical units (AU) from the sun], long exposures and complex sequences to compensate for image motion were required to obtain high-quality satellite images (most notably those of Miranda). Spacecraft engineering teams also redesigned the spacecraft's attitude control software to reduce random spacecraft motion. Image data compression was introduced to compensate for the low telemetry rates resulting from the large transmission distances. All of these efforts were successful and yielded many unsmeared, long-exposure images rich in details of the atmosphere and rings that would otherwise have remained unseen; they also provided some of the highest quality and highest resolution images of satellite surfaces acquired during any of the five Voyager encounters.

The Atmosphere of Uranus

Uranus is a low-contrast object. Variations in lighting and viewing angles cause about 95% of the brightness variation across the planet. Only after this dominant component is removed do the images reveal the underlying patterns that contain the fine

B. A. Smith, S. K. Croft, C. C. Porco, R. G. Strom, University of Arizona, Tucson, AZ 85721.
L. A. Soderblom, H. Masursky, J. B. Plescia, E. M. Shoemaker, U.S. Geological Survey, Flagstaff, AZ 86001.
R. Beebe, New Mexico State University, Las Cruces, NM 88003.
D. Bliss, R. H. Brown, S. A. Collins, C. J. Hansen, T. V. Johnson, S. P. Synnott, R. J. Terrile, Jet Propulsion Laboratory, California Institute of Technology, Pasadena, CA 91109.
J. M. Boyce and G. A. Briggs, NASA Headquarters, Washington, DC 20546.
A. Brahic, Observatoire de Paris, Meudon, Paris, France.
A. F. Cook II, Center for Astrophysics, Cambridge, MA 02138.
J. N. Cuzzi, J. B. Pollack, K. Rages, C. Stoker, NASA Ames Research Center, Moffett Field, CA 94035.
G. E. Danielson, T. E. Dowling, A. P. Ingersoll, California Institute of Technology, Pasadena, CA 91125.
M. E. Davies, Rand Corporation, Santa Monica, CA 90406.
D. Godfrey, C. Harris, G. E. Hunt, Imperial College, London, England.
R. J. Krauss, L. A. Sromovsky, V. E. Suomi, University of Wisconsin, Madison, WI 53706.
D. Morrison, University of Hawaii, Honolulu, HI 96822.
T. Owen, State University of New York, Stony Brook, NY 11794.
C. Sagan, P. Thomas, W. R. Thompson, J. Veverka, Cornell University, Ithaca, NY 14853.